Microglial IRF5-IRF4 regulatory axis regulates neuroinflammation after cerebral ischemia and impacts stroke outcomes

Abdullah Al Mamun[a], Anjali Chauhan[a], Shaohua Qi[a], Conelius Ngwa[a], Yan Xu[a], Romana Sharmeen[a], Amy L. Hazen[b], Jun Li[a], Jaroslaw A. Aronowski[a], Louise D. McCullough[a], and Fudong Liu[a,1]

[a]Department of Neurology, McGovern Medical School, The University of Texas Health Science Center at Houston, Houston, TX 77030; and [b]Institute of Molecular Medicine, McGovern Medical School, The University of Texas Health Science Center at Houston, Houston, TX 77030

Edited by Lawrence Steinman, Stanford University School of Medicine, Stanford, CA, and approved December 6, 2019 (received for review August 26, 2019)

Microglial activation plays a central role in poststroke inflammation and causes secondary neuronal damage; however, it also contributes in debris clearance and chronic recovery. Microglial pro- and antiinflammatory responses (or so-called M1-M2 phenotypes) coexist and antagonize each other throughout the disease progress. As a result of this balance, poststroke immune responses alter stroke outcomes. Our previous study found microglial expression of interferon regulatory factor 5 (IRF5) and IRF4 was related to pro- and antiinflammatory responses, respectively. In the present study, we genetically modified the IRF5 and IRF4 signaling to explore their roles in stroke. Both in vitro and in vivo assays were utilized; IRF5 or IRF4 small interfering RNA (siRNA), lentivirus, and conditional knockout (CKO) techniques were employed to modulate IRF5 or IRF4 expression in microglia. We used a transient middle cerebral artery occlusion model to induce stroke and examined both acute and chronic stroke outcomes. Poststroke inflammation was evaluated with flow cytometry, RT-PCR, MultiPlex, and immunofluorescence staining. An oscillating pattern of the IRF5-IRF4 regulatory axis function was revealed. Down-regulation of IRF5 signaling by siRNA or CKO resulted in increased IRF4 expression, enhanced M2 activation, quenched proinflammatory responses, and improved stroke outcomes, whereas down-regulation of IRF4 led to increased IRF5 expression, enhanced M1 activation, exacerbated proinflammatory responses, and worse functional recovery. Up-regulation of IRF4 or IRF5 by lentivirus induced similar results. We conclude that the IRF5-IRF4 regulatory axis is a key determinant in microglial activation. The IRF5-IRF4 regulatory axis is a potential therapeutic target for neuroinflammation and ischemic stroke.

brain | interferon regulatory factor | microglia | neuroinflammation | stroke

Innate immune responses play a critical role in the progress of cerebral ischemic injury and contribute to secondary neuronal damage (1). Although the poststroke inflammation exacerbates the injury, the ischemic brain also needs the inflammatory response to help clear debris and promote tissue repair. Therefore, the immune response has dual effects in stroke depending on the timing and site of activation. Overall suppression of the immune response has resulted in adverse side effects both clinically and experimentally (2–4). Microglia, the resident immune cells in the brain, play a central role in initiating and perpetuating the immune response (5). These cells are well known to have 2 activation states after pathogenic stimulation that lead to either a pro- or an antiinflammatory phenotype, often classified as "M1 and M2," respectively, depending on the inflammatory environment (6). Although it is increasingly recognized that this binary classification is an oversimplified characterization of microglial activation as the 2 states seem to overlap during disease progress, either of the 2 predominates at different stages of the disease. In fact, it has been demonstrated that the depletion of microglia exacerbates postischemic inflammation and brain injury in young mice (7, 8), suggesting that microglia are needed to reduce ischemic injury and are not exclusively neurotoxic. Nevertheless, what drives microglia to polarize to different activation states after stroke remains unknown. It has high translational value to manipulate microglial activation by suppressing their M1 and/or boosting their M2 phenotype to limit inflammatory damage and promote tissue repair.

Interferon regulatory factors (IRF) mediate macrophage activation in peripheral immune cells and other inflammatory diseases (9). Our previous studies have shown that IRF5 and IRF4 expression in microglia exhibited a "see-saw" pattern and corresponded with pro- and antiinflammatory profiles, respectively, after stroke (10). The results strongly suggest that the IRF5-IRF4 signaling forms a regulatory axis to balance microglial pro- and antiinflammatory activation. We hypothesize that IRF5 signaling mediates microglial proinflammatory responses and that IRF4 signaling favors microglial antiinflammatory activation, and as a result, the IRF5-IRF4 regulatory axis impacts stroke outcomes. In the present study, we utilized genetic methods to manipulate the IRF5-IRF4 regulatory axis in animal models to explore the mechanisms underlying the dual effects of the immune response to stroke.

Results

Microglial IRF5 and IRF4 Expression Corresponded to Different Profiles of Cytokine Production in an Oxygen-Glucose Deprivation Model. Since microglia are activated toward either pro- or antiinflammatory phenotypes after stroke, manipulation to suppress the

Significance

Cerebral ischemia is a powerful stimulus to induce pro- and antiinflammatory responses, with the former destructive and the latter reparative in the disease progress. Microglia, the resident immune cells in the brain, are the key cells in initiating and perpetuating the poststroke inflammation. If microglial activation after stroke can be controlled, the poststroke inflammation will be quenched and stroke outcomes improved. In this study, we identified a key determinant for microglial pro- and antiinflammatory activation, the IRF5-IRF4 regulatory axis. We demonstrated that the manipulation of the axis alters stroke outcomes. This is an important finding, as the IRF5-IRF4 regulatory axis potentially provides stroke scientists with a therapeutic target for the treatment of stroke.

Author contributions: J.L., J.A.A., L.D.M., and F.L. designed research; A.A.M., A.C., S.Q., C.N., Y.X., R.S., and F.L. performed research; A.L.H. contributed new reagents and analytic tools; A.A.M. analyzed data; and A.A.M. and F.L. wrote the paper.

The authors declare no competing interest.

This article is a PNAS Direct Submission.

[1]To whom correspondence may be addressed. Email: fudong.liu@uth.tmc.edu.

This article contains supporting information online at https://www.pnas.org/lookup/suppl/doi:10.1073/pnas.1914742117/-/DCSupplemental.

First published December 31, 2019.

M1 and/or promote M2 response should attenuate poststroke inflammation and benefit outcomes. To test if microglia phenotypes can be manipulated, we started with in vitro assays. Primary microglia cultures were exposed to oxygen-glucose deprivation (OGD), an in vitro ischemia model, and then stimulated with lipopolysaccaride (LPS) or IL-4 to induce different microglial activation (11, 12). Normoxia served as a "sham" control to OGD. As expected, OGD+LPS stimulation induced a lower ratio of IRF4-IRF5 expression compared with normoxia, indicating a relatively higher expression of IRF5 than IRF4 (Fig. 1 *A* and *B*). However, OGD+IL-4 stimulation elicited a similar ratio of IRF4-IRF5 (≥1) as in the normoxic condition, suggesting IRF4 predominant expression. RT-PCR was performed in cell homogenates to measure messenger RNA (mRNA) levels of cytokines. Proinflammatory mRNA levels [iNOS, tumor necrosis factor-alpha (TNFα), CD68, MHCII] were significantly higher in OGD+LPS– vs. OGD+IL-4–stimulated microglia, consistent with a M1 profile (Fig. 1 *C–F*). In contrast, antiinflammatory (M2) mRNA levels (CD206, IL-10, Arginase1, TGFβ) were higher in OGD+IL-4 vs. OGD+LPS microglia (Fig. 1 *G–J*). These data indicate that, under different stimulations, IRF5-IRF4 signaling varies and microglial phenotypes can be changed.

Knockdown of IRF5 and IRF4 in Primary Cultured Microglia Led to Increased Expression of IRF4 and IRF5, Respectively. Next, we tested if the IRF5-IRF4 regulatory axis can be modified to switch microglial phenotypes between M1 and M2. We applied IRF4 or IRF5 small interfering RNA (siRNA) to the primary microglial culture to down-regulate IRF4 or IRF5 protein expression and then exposed the culture to OGD. IRF4 and IRF5 siRNAs induced significant lower expression of of their target proteins respectively in cultured microglia under normoxic conditions compared to the scrambled siRNA; however, interestingly, IRF5 siRNA caused higher expression of IRF4, and IRF4 siRNA led to higher IRF5 under OGD conditions (Fig. 2 *A–F*). Cytokine levels were also examined in the cell-culture medium. For the proinflammatory cytokine TNFα, OGD induced significantly higher levels than normoxia in each siRNA-treated cell dish, and IRF4 siRNA-treated medium had higher levels than IRF5 or scramble siRNA medium (Fig. 2*H*). For the antiinflammatory cytokine IL-4, OGD induced significantly higher levels only in IRF5 siRNA-treated cells (Fig. 2*G*). These in vitro experiments suggested that IRF5 and IRF4 signaling inhibit each other and that the manipulation of the IRF5-IRF4 regulatory axis leads to a microglial phenotype switch.

Conditional Knockout of IRF5 and IRF4 Induced Microglial Pro- and Antiinflammatory Responses, Respectively, after Stroke. Inspired by the in vitro results, we set out to test our hypothesis with in vivo assays.

We created an IRF5 or IRF4 conditional knockout (CKO) animal model by crossing IRF5 or IRF4 floxed mice with lysozyme M (LysM) Cre mice. LysM is a marker for monocytic cells (13, 14),

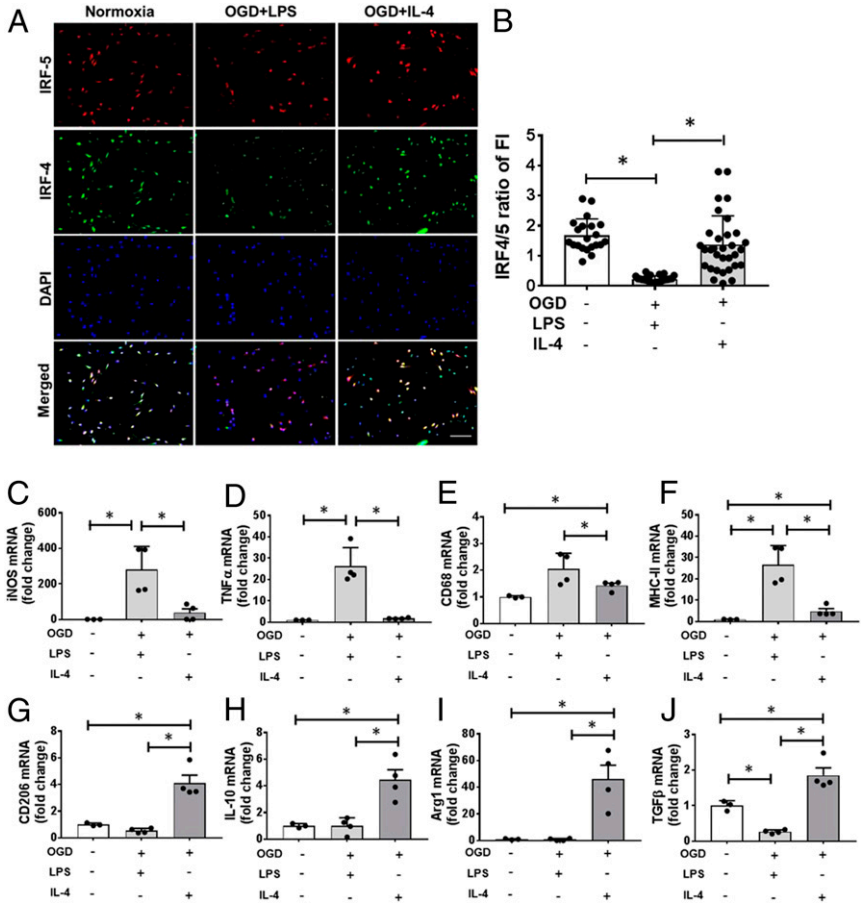

Fig. 1. Microglial IRF5-IRF4 expression and phenotypes after OGD. (*A*) ICC of primary microglia exposed to OGD+LPS or +IL-4 stimulation showing IRF5 and IRF4 expression. 20×; (Scale bar, 100 μm.) (*B*) Ratio of IRF4 over IRF5 fluorescence intensity (FI). Data were averaged from 21 to 24 microscopic fields from 3 independent experiments; each dot represents the FI of one 20× microscopic field. *$P < 0.05$. (*C–F*) Proinflammatory mRNA levels by RT-PCR in cultured microglia. (*G–J*) Anti-inflammatory mRNA levels in microglia. Data were averaged from 3 to 4 independent experiments; each dot represents the mRNA level from one independent experiment. *$P < 0.05$.

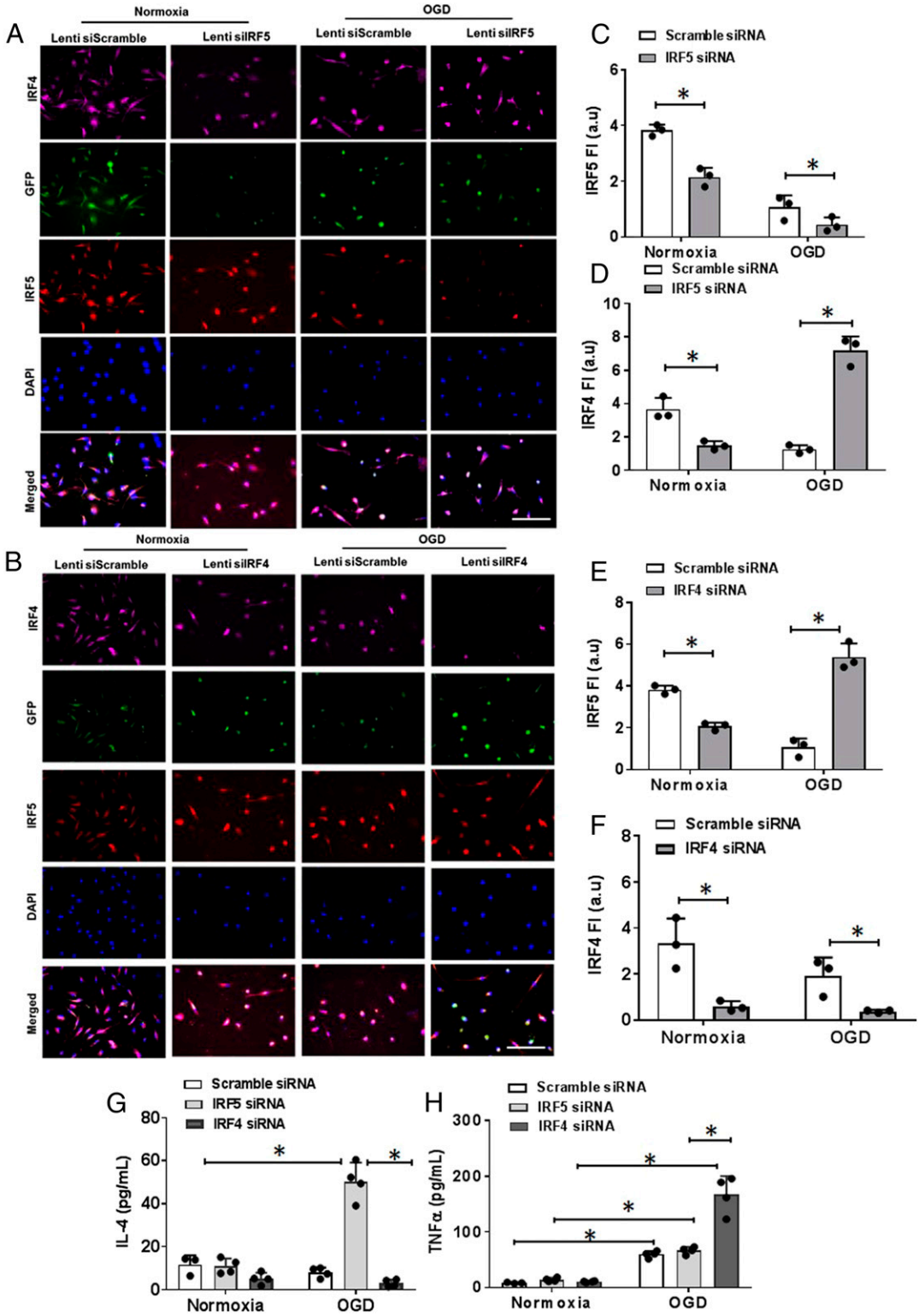

Fig. 2. IRF5-IRF4 expression and cytokine levels in siRNA/OGD-treated microglia cultures. (*A* and *B*) ICC staining of IRF5-IRF4 in IRF5 siRNA- (*A*) and IRF4 siRNA- (*B*) treated microglia. 40×; (Scale bar, 100 μm.) (*C–F*) IRF5-IRF4 fluorescence intensity in IRF5 siRNA- (*C* and *D*) and IRF4 siRNA- (*E* and *F*) treated microglia. (*G* and *H*) IL-4 and TNFα levels by ELISA in cell-culture medium. Data were averaged from 3 independent experiments with duplicate wells, and each dot represents the average FI of 12 to 16 random 40× microscopic fields. *$P < 0.05$.

and lysozyme M-Cre (LysMCre) mice have been widely used to target genes of interest in microglia (15–17). We have validated our IRF CKO mouse model by performing RT-PCR in flow-cytometry–sorted microglia for IRF mRNA levels, and microglia of the CKO mice had "near null" IRF5 or IRF4 mRNA levels compared to control mice (IRF5-4 gene floxed mice) (*SI Appendix*, Fig. S1). Young male IRF5 or IRF4 CKO mice (8 to 12 wk) were subject to a 60-min middle cerebral artery occlusion (MCAO)

model. Three days after MCAO, flow cytometry was conducted to examine microglial phenotypes by examining the cell membrane and intracellular inflammatory markers. The gating strategy for microglia and other immune cells is indicated in *SI Appendix*, Fig. S2. CD68 and CD206 are well-validated cell-membrane pro- and antiinflammatory markers, respectively (18, 19), whereas IL-1β-TNFα and IL-4/IL-10 are considered intracellular pro- and anti-inflammatory cytokines (20, 21). After MCAO, IRF5 CKO microglia exhibited significantly higher expression levels of the cell-membrane marker CD206 and lower levels of CD68 compared to control microglia (Fig. 3 *A*–*C*); in contrast, IRF4 CKO resulted in low CD206 and high CD68 levels in microglia (Fig. 3 *D*–*F*). For intracellular inflammatory mediators, IRF5 CKO microglia had a significantly lower level of TNFα and a higher level of IL-10 compared to the control after stroke, although the changes in IL-1β and IL-4 levels were not significant (Fig. 4 *A*–*F*). More dramatic changes were seen in IRF4 CKO microglia, as levels of both antiinflammatory cytokines (IL-4/IL-10) were significantly lower in CKO vs. control microglia after stroke, and levels of both proinflammatory cytokines (IL-1β/TNFα) were significantly higher in CKO vs. control stroke mice (Fig. 4 *G*–*L*). These data indicate that CKO of IRF5 or IRF4 changed microglial phenotypes after stroke, which exhibited an oscillating pattern. Surprisingly, we did not find any significant difference in CD68 or CD206 expression on infiltrating monocytes between IRF5 or IRF4 CKO vs. floxed mice (*SI Appendix*, Fig. S3), suggesting a more important role of the IRF5-IRF4 regulatory axis in microglia vs. infiltrating monocytes in stroke brains.

Peripheral Immune Responses Were Different in IRF5 vs. IRF4 CKO Stroke Mice. We also examined peripheral immune-cell infiltration in the brain and plasma cytokine levels to evaluate the peripheral immune response 3 d after stroke. Flow cytometry data showed that IRF4 CKO had significantly more leukocytes, including total peripheral myeloid cells (pMyeloid), monocytes, and neutrophils, infiltrating into the stroke brain compared to the control group (Fig. 5 *A*–*D*). IRF5 CKO failed to induce any significant difference in the infiltration of peripheral immune cells compared to floxed mice after stroke (*SI Appendix*, Fig. S1). MultiPlex was performed in the plasma of all mice to measure cytokine levels. IRF4 CKO significantly increased plasma levels of the proinflammatory cytokines TNFα, IL-12, and IL-6 (Fig. 5 *J*–*M*). Although IRF5 CKO caused minimal changes in peripheral immune cell infiltration, the mutation decreased plasma TNFα and granulocyte-colony–stimulating factor (G-CSF) levels and induced a decreasing trend in IL-1β (Fig. 5 *F*–*I*), all of which are

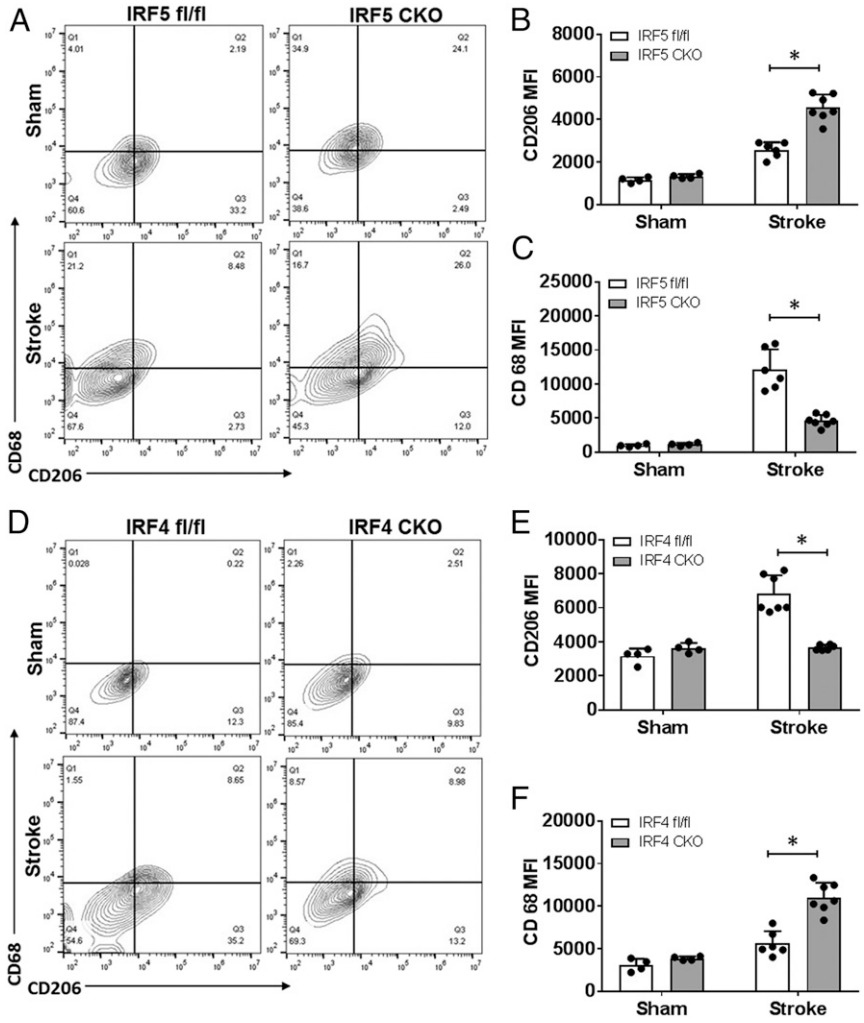

Fig. 3. Cell-membrane inflammatory marker levels in IRF5 or IRF4 CKO microglia by flow cytometry performed on stroke and sham brains. (*A* and *D*) Representative flow plots of IRF5 (*A*) and IRF4 (*D*) CKO microglia gated by CD68 and CD206. Quantification data were presented as MFI. The MFI of CD206 and CD68 is shown in *B* and *C* for IRF5 CKO and in *E* and *F* for IRF4 CKO microglia. $n = 4$ to 5 per sham and 6 to 7 per stroke group; $^*P < 0.05$.

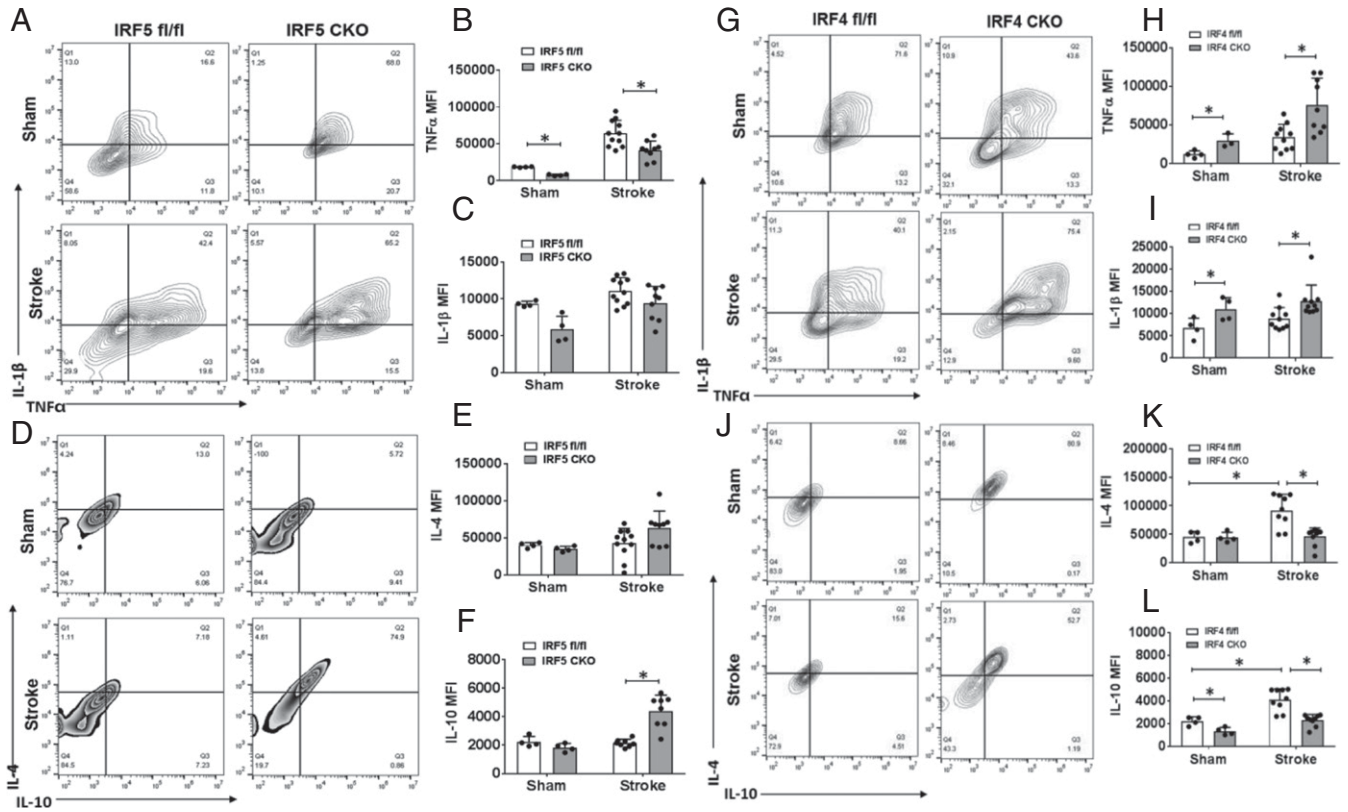

Fig. 4. Intracellular cytokine levels in IRF5 or IRF4 CKO microglia by flow cytometry performed on stroke and sham brains. Quantification data are presented as mean MFI. (*A–L*) Data of IRF4 and IRF5 CKO microglia, respectively. *A*, *D*, *G*, and *J* are representative intracellular staining plots for TNFα/IL-1β and IL-4/IL-10. MFI of these cytokines were quantified in *B–F* for IRF5 CKO and in *H*, *I*, *K*, and *L* for IRF4 CKO microglia. $n = 4$ to 5 per sham and 6 to 7 per stroke group; $^*P < 0.05$.

considered proinflammatory. Given that IRF5 CKO had more dramatic effects on microglial activation (Fig. 4) vs. peripheral leukocyte infiltration (*SI Appendix*, Fig. S4), the plasma cytokine level changes caused by IRF5 CKO may reflect an effect of microglia on cytokine release. The neuroinflammation data from Figs. 4 and 5 indicate that CKO of IRF5 or IRF4 not only can switch microglial phenotypes, but also has effects on peripheral immune responses, suggesting a control role of the IRF5-IRF4 regulatory axis in poststroke inflammation.

CKO of IRF5 and IRF4 Have Opposite Effects on Stroke Outcomes. To evaluate the role of the IRF5-IRF4 regulatory axis in stroke outcomes, we examined stroke outcomes in IRF5 or IRF4 CKO mice after MCAO at both acute (3 d) and chronic (30 d) phases. Both CKO and control mice were subjected to a 60-min MCAO; histological outcomes and sensorimotor/cognitive deficits were quantified. After 3 d of stroke, IRF5 CKO mice had significantly smaller infarct in each brain area (cortex, striatum, ipsilateral hemisphere) than control mice (Fig. 6*A*), and they had better behavioral outcomes in the hanging wire (Fig. 6*C*) and corner test (Fig. 6*D*). Although IRF4 CKO mice had larger infarct only in the striatum (Fig. 6*I*) at 3 d, behavioral deficits were significantly worse in the neurological deficit score (NDS) (Fig. 6*K*), corner test (Fig. 6*L*), and tape removal test (Fig. 6 *M* and *N*). Brain atrophy was measured at 30 d of MCAO for histological changes after stroke, as the infarct tissue has been cleared at the chronic stage. Although the brain atrophy was not significantly different in brains of IRF5 CKO vs. flox stroke mice (Fig. 6*B*), the CKO mice did have better outcomes in the tape removal test (Fig. 6 *E* and *F*). IRF4 CKO mice had significantly more brain-tissue loss compared to their controls, and they also suffered more from sensorimotor deficits (corner test in Fig. 6*L*; tape removal test in Fig. 6 *M* and *N*) and cognitive deficit (novel object recognition test in Fig. 6*P*) than their control counterparts. In summary, these data clearly show IRF5-IRF4 signaling in myelomonocytic cells had a detrimental/beneficial effect, respectively, on stroke outcomes.

Lenti-IRF5 Treatment Exacerbated Proinflammatory Response to Stroke. To further test our hypothesis that the microglial IRF5-IRF4 regulatory axis is critical to poststroke neuroinflammation, and directly manipulate central (brain) signaling, we injected IRF5 or IRF4 lentivirus in vivo to overexpress IRF5 or IRF4 protein in microglia prior to stroke. The lenti-IRF5 or -IRF4 virus was conjugated with CX3CR1 promoter and injected intracortically and intrastriatally 4 wk before MCAO, leading to selective IRF protein overexpression in microglia, as CX3CR1 is expressed exclusively in microglia in brain tissue (22–24). The lentiviruses led to overexpression of target proteins that was 5 times higher than that of the lenti-GFP control evaluated by mRNA levels through RT-PCR assays on flow-sorted microglia (*SI Appendix*, Fig. S5). To confirm if overexpression of IRF5/IRF4 can change microglial phenotypes, we again conducted flow cytometry on ischemic brain samples to examine microglial activation at 3 d of MCAO. Lenti-IRF5–treated microglia exhibited significantly less CD206 expression compared to lenti-IRF4 treatment (Fig. 7 *A* and *C*); the mean fluorescence intensity (MFI) of the proinflammatory marker CD68 was significantly higher in lenti-IRF5– vs. -IRF4–treated microglia after stroke (Fig. 7 *A* and *B*). For the expression of the intracellular proinflammatory marker TNFα, lenti-IRF5 induced a significantly higher level than lenti-IRF4 in stroke groups (Fig. 7 *D* and *E*). Both viruses led to increased TNFα after stroke compared

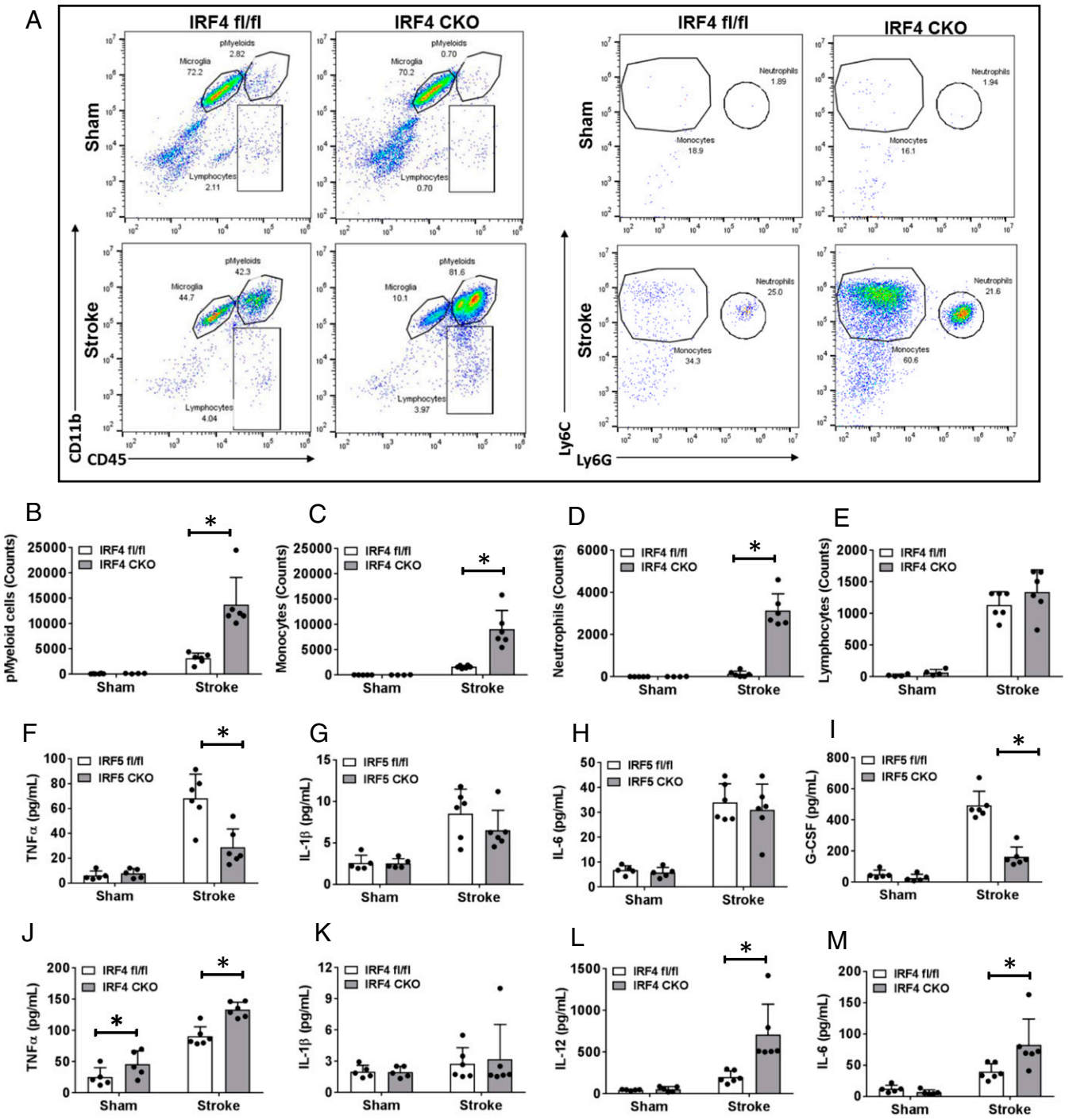

Fig. 5. Brain infiltration of peripheral immune cells and circulating cytokine levels in IRF5 or IRF4 CKO mice. (*A*, *Left*) Flow plots: representative gating plots for total pMyeloid, microglia, and lymphocytes. (*A*, *Right*) Flow plots: gating strategy for monocytes and neutrophils. (*B*) Percentage of pMyeloid cells. (*C–E*) Absolute cell counts of monocytes (*C*), neutrophils (*D*), and lymphocytes (*E*). (*F–M*) Plasma levels of cytokines in IRF5 and IRF4 CKO mice, respectively. $n = 5$ to 6 per sham and 6 to 7 per stroke group; $^*P < 0.05$.

to shams, reflecting an effect of virus itself. After MCAO, the lenti-IRF5–treated group had significantly more leukocyte infiltration (pMyeloid cells, monocytes, and neutrophils) than the lenti-IRF4–treated group (Fig. 7 *F–H*).

Overexpression of IRF5 and IRF4 in Microglia Was Sufficient to Impact on Stroke Outcomes. Since lenti-IRF5 treatment amplified the microglial proinflammmatory (M1) phenotype, we next evaluated if the enhanced microglial M1 phenotype had any impact on stroke outcomes. Three days after MCAO, behavioral deficits and infarct volumes were quantified. Compared to the lenti-GFP–injected group, lenti-IRF5 induced a significantly larger infarct in the ipsilateral hemisphere. Overexpression of IRF4, however, led to significant neuroprotection in the cortex (Fig. 8 *A* and *B*). Overexpression of Lenti-IRF5 led to worse behavioral deficits in the NDS (vs. lenti-GFP or -IRF4) and corner test (vs. lenti-IRF4) (Fig. 8 *C* and *D*), with no significant effect on the hanging wire test (Fig. 8*E*).

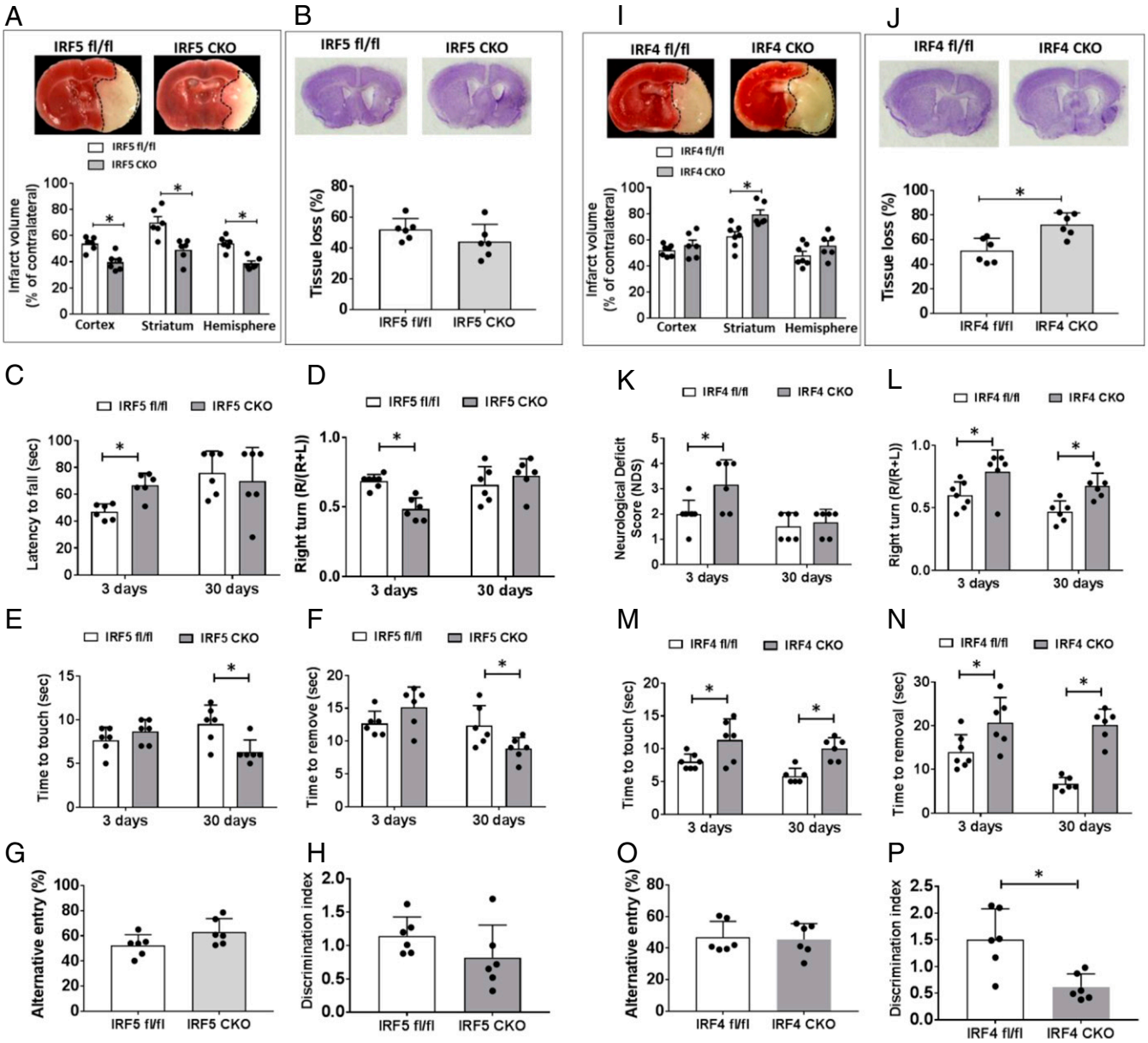

Fig. 6. Stroke outcomes from IRF5 and IRF4 CKO mice after MCAO. (*A* and *I*) Representative images of TTC-stained brain slices and quantification of infarct size in IRF5 (*A*) and IRF4 (*I*) CKO mice brains at 3 d of MCAO. (*B* and *J*) Representative images of CV-stained brain slices and quantification of tissue loss in IRF5 (*B*) and IRF4 (*J*) CKO mice brains at 30 d of MCAO. For IRF5 CKO mice, hanging wire test (*C*), corner test (*D*), and tape removal test (*E* and *F*) were performed at 3 d and 30 d after stroke; Y-maze (*G*) and NORT (*H*) were tested only at 30 d. For IRF4 CKO group, NDS (*K*), corner test (*L*), and tape removal test (*M* and *N*) were performed at both acute and chronic stages of stroke; Y-maze (*O*) and NORT (*P*) were tested only at 30 d. $n = 6$ to 7 per group; $^*P < 0.05$.

Discussion

Microglia are the resident immune cells in the brain and play a fundamental role in mediating poststroke neuroinflammation (6). To a large extent, the microglial response shapes poststroke inflammation and significantly contributes to ischemic pathophysiology. It is well known that microglia are activated toward pro- and antiinflammatory phenotypes after brain injury (5); however, the molecular pathways through which microglia are differently activated remains elusive. This report examines the role of the IRF5-IRF4 regulatory axis in the microglial response and also the transgenic methodologies to mechanistically investigate the pro- and antiinflammatory pathways underlying microglial activation. A previous study by Lively and Schlichter (25) reported that microglial responses to proinflammatory stimuli (LPS, IFNγ+TNFα) can be reprogrammed by resolving cytokines (IL-4, IL-10) to exhibit the M2 phenotype. However, this study used only pathogen stimulation to examine microglial phenotypes, and how these stimuli or cytokines program microglial activation has never been reported.

The most important findings of the present study are that the IRF5 signaling directs the microglial proinflammatory response and that IRF4 signaling affects microglial antiinflammatory activation. IRFs have been found to play pivotal roles in peripheral macrophage activation after inflammatory insults (9). Our previous study demonstrated a high expression of IRF5 acutely, followed by a chronic increase in IRF4, which was accompanied by robust expression of pro- and antiinflammatory cytokines, respectively (10). The see-saw pattern of IRF5-4 expression and M1-M2 microglial phenotypes led us to test if the IRF5-IRF4 regulatory axis is a major player in microglial activation. Microglia represent the first line of defense against ischemic stroke, and we

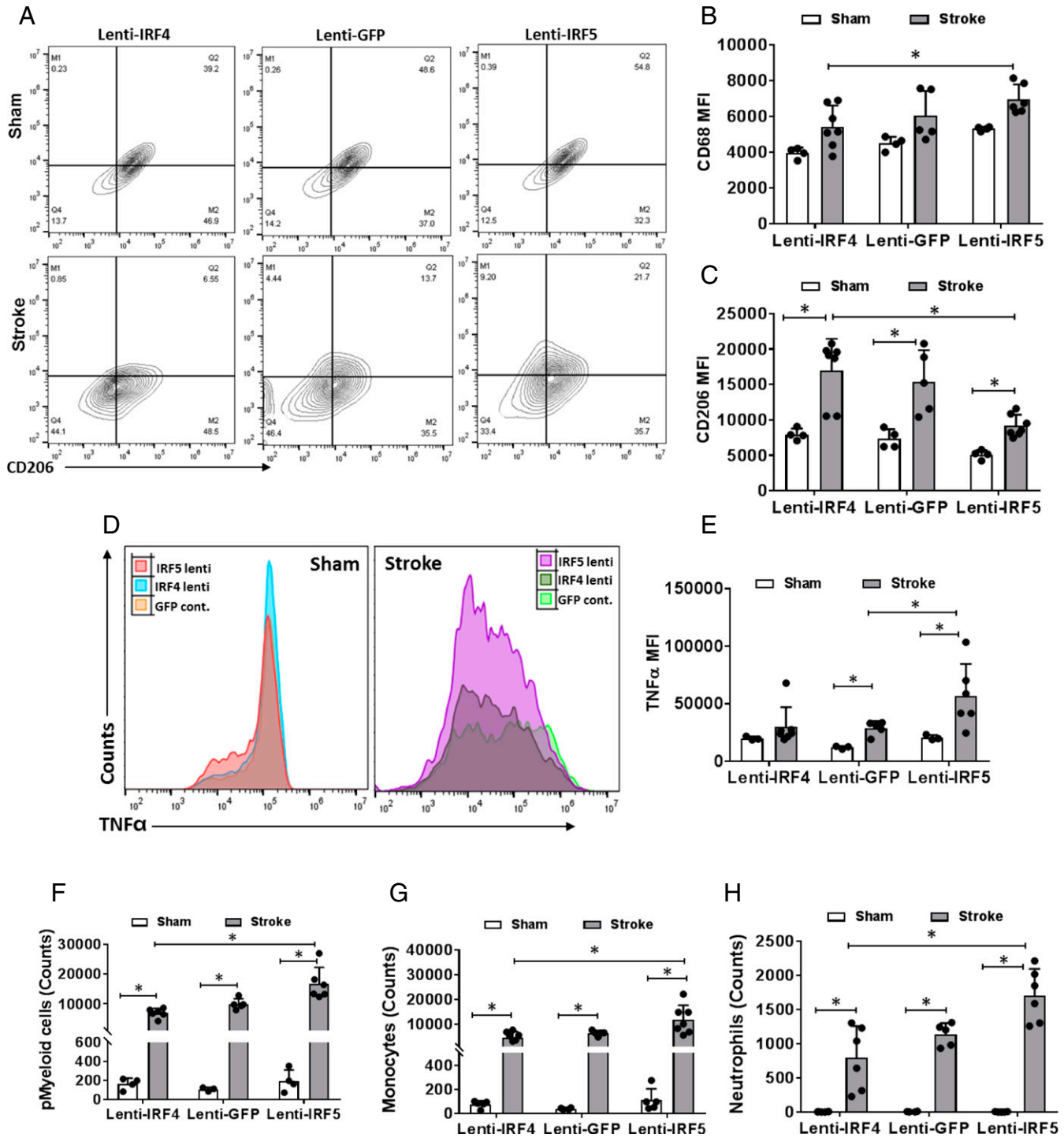

Fig. 7. Microglial activation and peripheral immune cell infiltration in IRF5 or IRF4 lentivirus-treated C57BL/6 mice brains after stroke. Lenti-GFP served as a control lentivirus for lenti-IRF5 and -IRF4. (*A*) Representative flow plots of CD68/CD206-gated microglia from lenti-IRF5/-IRF4–treated mice. (*B* and *C*) Quantification of CD68 (*B*) and CD206 (*C*) MFI in lenti-IRF5/-IRF4–treated microglia. (*D*) Representative histogram plots for intracellular TNFα expression in lentivirus-treated microglia. (*E*) Quantification of TNFα MFI in *D*. (*F*–*H*) Absolute cell counts of infiltrating pMyeloid cells (*F*), monocytes (*G*), and neutrophils (*H*) in lentivirus-treated mice brains after stroke. $n = 5$ for Lenti-GFP control and 6 for the lenti-IRF4 or -IRF5 group; $^*P < 0.05$.

wanted to selectively target this important component of the inflammatory response without altering the entire immune system. Unlike other acute pathological changes (oxidative stress, calcium overloading, etc.), the immune response to ischemic injury peaks later and lasts for months poststroke (26, 27), providing us with a longer time window to intervene to potentially improve stroke outcomes. The progress of the inflammatory response is very dynamic and the pro- and antiinflammatory responses are intricately tied to each other throughout disease progression, as shown in previous studies (5, 10, 28). Total depletion of proliferative microglia has been reported to worsen ischemic brain damage (3, 4), which is not surprising based on our results, as this method

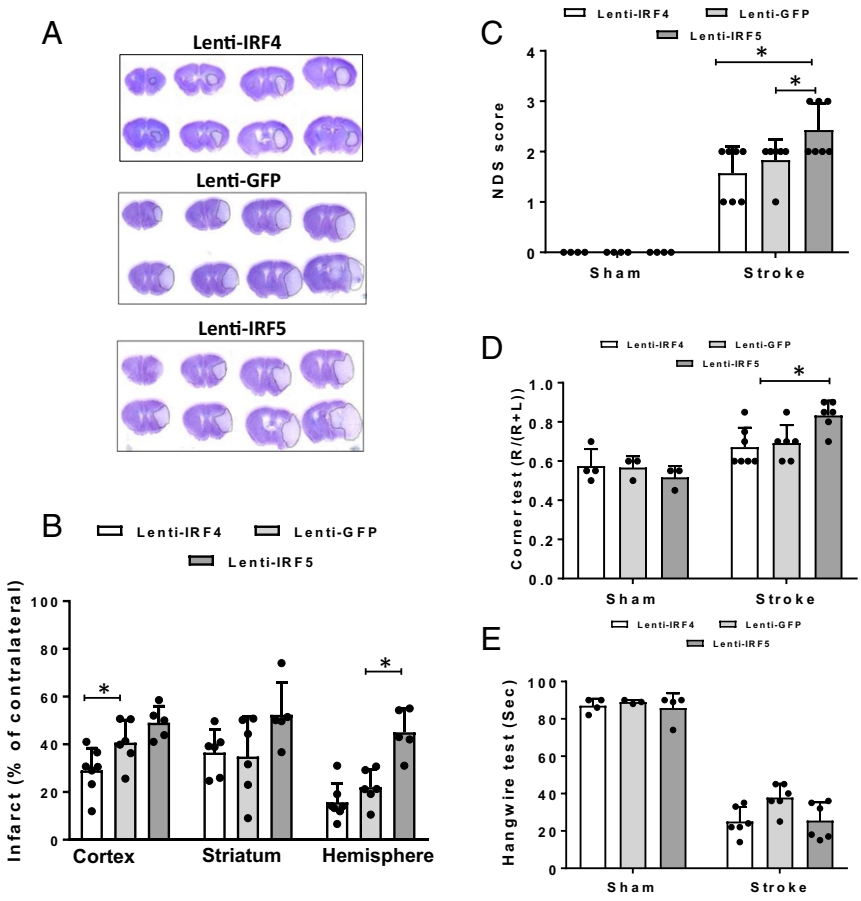

Fig. 8. Stroke outcomes from lentivirus-treated C57BL/6 mice after MCAO. (*A*) Representative images of CV-stained brain slices from lenti-IRF5/-IRF4–treated mice. (*B*) Quantification of infarct size in *A*. (*C*–*E*) Behavioral deficit data in the NDS (*C*), corner test (*D*), and hanging wire test (*E*) for lenti-IRF5/-IRF4–treated mice. $n = 5$ for Lenti-GFP control and 6 for lenti-IRF4 or -IRF5 group; $^*P < 0.05$.

eliminates all microglial functions including their M2-related reparative capability.

Both in vitro and in vivo data in the present study showed that microglial M1-M2 phenotypes appear to be quite malleable and can be changed and switched if IRF5-IRF4 expression levels are manipulated. If microglial IRF5 expression is suppressed, IRF4 expression levels increase, and vice versa in the case of IRF4 down-regulation. The oscillating pattern of IRF5-IRF4 expression suggests that there is an unknown endogenous inhibitory pathway that acts on IRF5 or IRF4 once its counterpart is more active. In addition, microglial production of brain pro- or antiinflammatory cytokines is also changed accordingly to reflect the predominate IRF signaling, IRF5 or IRF4 (Figs. 3, 4, and 7). This also affects the infiltration of peripheral immune cells and the circulating levels of cytokines (Figs. 5 and 7). This can be explained by the competition of IRF5 with IRF4 for binding to the adaptor protein MyD88, a key component of the phosphorylation complex that also includes TNF receptor-associated factor 6, interlukin-1 receptor-associated kinase 1 (IRAK 1) and IRAK 4 (29, 30). If IRF4 signaling predominates, IRF4 binds to MyD88, leading to a subsequent decrease in IRF5 phosphorylation, less activated IRF5, and lower expression of proinflammatory mediators. Our data clearly point to the importance of the microglia response in the poststroke inflammation and also suggest that the microglial IRF5-IRF4 regulatory axis can be potentially used as a clinical target to treat ischemic stroke and other neuroinflammatory diseases. Cell-specific therapy has been very promising due to the rapid development of lentiviral vectors and siRNA techniques (31, 32) and represents a therapeutic avenue due to their ability to more precisely target cell-specific signaling pathways, avoiding more global changes in immune regulation. Based on our results, pharmacological reagents could be developed to decrease IRF5 and/or increase IRF4 expression in microglia after stroke, so that the proinflammatory response can be inhibited and the antiinflammatory response induced earlier to clear the ischemic debris and boost the tissue repair.

The characterization of microglial M1-M2 phenotypes is recognized as an oversimplified conceptual framework that refers to 2 distinctive and extreme activation states (27). M1 or M2 activation can coexist in a single microglia, and there is a continuum of mixed expression of M1 and M2 rather than an "all or none" phenomenon. This has been demonstrated by previous studies (5, 33) and was confirmed in the present study showing microglia coexpress pro- and antiinflammatory cytokines (Figs.1–5 and 7). Nevertheless, the coexpression was not equal, and 1 of the 2 activation states predominated when IRF5 or IRF4 was manipulated. Therefore, the broad M1 and M2 classification is still useful, as it exemplifies the dynamic microglial response to brain injuries and helps to understand the functional status of microglia (27). Emerging literature has reported changes in microglial M1-M2 phenotypes in various neuroinflammatory diseases, including Alzheimer's disease (34), multiple sclerosis (35), traumatic brain injury (36), and stroke (37), all of which indicate the importance of changes in microglial M1-M2 polarization and expand the potential importance of this study.

All experiments of the project were designed to specifically target microglial IRF5-IRF4 signaling, except the CKO stroke outcome data (Fig. 6) generated by using the animal model that was derived from a cross between IRF floxed and LysMCre mice. LysMCre will lead to deletion of floxed genes not only on microglia

but also on monocytes, which is a caveat of the present study. However, we specifically analyzed microglial/monocytic M1-M2 markers with flow cytometry in IRF5 or IRF4 CKO mice and found only an alteration in M1/M2 states in microglia but not in monocytes (*SI Appendix*, Fig. S3), suggesting that the IRF5-IRF4 regulatory axis may not play a key role in the polarization of infiltrating monocytes in stroke brains. To date, microglia specifically targeted Cre mice are not available. To further distinguish the roles of IRF5/IRF4 signaling in microglia vs. monocytes, ongoing experiments in the A.A.M. laboratory are using bone marrow chimera (38) and inducible CKO based on CX3CR1-CreER mice (39) to separately examine monocyte vs. microglial responses. Nevertheless, the present study conducted multiple assays using different technology (in vitro siRNA, in vivo CKO, and lentiviruses), each of which has yielded similar results and strongly support our hypothesis.

In summary, our study has revealed a determinant mechanism underlying microglial activation, i.e., the IRF5-IRF4 regulatory axis. By manipulation of IRF5/IRF4 expression in microglia, we demonstrated an oscillating pattern of the IRF5-IRF4 regulatory axis that controlled microglial M1/M2 phenotypes and the pro- and antiinflammatory responses to stroke. Altering the balance of the IRF5-IRF4 regulatory axis had a significant impact on stroke outcomes at both acute and chronic stages, indicating a pivotal role of IRF5-IRF4 signaling in mediating ischemic injury. Importantly, since microglial activation is ubiquitous in various neurodegenerative and neuroinflammatory diseases, the mechanistic action of the IRF5-IRF4 regulatory axis could also exist in other brain disorders. As the nondiscriminatory intervention of microglial activation has proven detrimental, our finding of the microglial IRF5-IRF4 regulatory axis provides a precise and effective therapeutic target for poststroke inflammation and ischemic injury and potentially for many other central nervous system diseases.

Methods

Experimental Animals. All animal protocols were approved by the University of Texas Institutional Animal Care and Use Committee and were performed in accordance with NIH and University of Texas Health Science Center at Houston (UTHealth) animal guidelines. C57BL/6 young male mice (8 to 12 wk; Jackson Laboratory) were used for lentivirus injection. IRF4 or IRF5 fl/fl mice were crossed with LysMCre mice (Jackson Laboratory) to obtain microglial CKO. All adult mice were group-housed under pathogen-free conditions with a 12- to 12-h day–night cycle and had access to food and water ad libitum.

Primary Mixed Glial Cultures. Primary cortical mixed glial cultures were prepared from C57BL/6 mouse brains within 0 to 2 d of birth as in ref. 40. Briefly, the cortices were dissociated via serial incubations with neuronal dissociation kit according to the manufacturer's instruction (MACS Miltenyi Biotech). The mixed cells were cultured in Dulbecco's Modified Eagle Media supplemented with 10% fatal bovine serum and 1% penicillin/streptomycin for 10 d at 37 °C and 5% CO_2. The culture was boosted by replacing L929-conditioned media at days 3 and 5. After 10 d, flasks were shaken for 3 h at 300 × *g* to remove loosely attached microglia. The collected microglia were further cultured in 8-well chamber slides for immunocytochemistry (ICC) and in 6-well plate coated with poly-D-lysine (0.001%, Sigma) for gene expression analysis. The purity of these microglial cultures was 99% as determined by Iba1 immunoreactivity.

OGD and siRNA/Short Hairpin RNA Lentivirus Transfection. To model ischemia/reperfusion conditions in vitro, the microglia cultures were exposed to OGD as described previously (41). The culture medium was replaced with serum-free, glucose-free Locke's buffer (154 mM NaCl, 5.6 mM KCl, 2.3 mM CaCl2, 1 mM MgCl2, 3.6 mM NaHCO3, 5 mM Hepes and 5 mg/mL gentamicin, pH 7.2), and the cultures were incubated in an experimental hypoxia chamber in a saturated atmosphere of 95% N2 and 5% CO_2 for 8 h. The control cells were cultured in the presence of normal levels of glucose and were incubated in a humidified atmosphere of 95% air and 5% CO_2. After 8 h of OGD, cultured microglia were treated with LPS (100 μg/mL) or IL-4 (20 ng/mL) for M1 or M2 stimulation, respectively. For efficient IRF4 and IRF5 knockdown in primary microglia by siRNA, we have used iLenti RNAi Expression System (abm Biotech) as described in refs. 42 and 43. The siRNA-treated cells were subject to 4-h OGD.

ICC. Cultured cells were fixed with 4% paraformaldehyde for 30 min at room temperature, washed with 0.1 M Tris-buffered solution (TBS; pH 7.5), blocked with 3% donkey serum (Sigma) in TBS containing 0.3% Triton X-100 at room temperature for 60 min, and incubated overnight with the mouse and goat primary antibody against IRF4 (sc-6059, Santa Cruz Biotechnology, Dallas, TX) and IRF5 (sc-56714, Santa Cruz Biotechnology) at 4 °C. The cells were then washed with TBS and incubated with either Alexa Fluor 594- or 647-conjugated secondary antibody (1:1,000; Invitrogen, Carlsbad, CA) for 60 min. Finally, stained cells were mounted with Fluoroshield with DAPI (#F6057, Sigma) and visualized using a Leica DMi8 confocal microscopy (Buffalo Grove, IL). Images were processed using ImageJ software (NIH). The fluorescence intensity of IRF4 and IRF5 immunoreactivity was measured in 21 to 24 random microscopic fields from 3 independent experiments by a blinded investigator.

Ischemic Stroke Model. Cerebral ischemia was induced by 60-min reversible MCAO under isoflurane anesthesia as previously described (44). Rectal temperature was maintained at 36.5 ± 0.5 °C during surgery with an automated temperature-control feedback system. A midline ventral neck incision was made, and unilateral MCAO was performed by inserting a 6.0-mm monofilament (Doccol, Redlands, CA) into the right internal carotid artery 6 mm from the internal carotid/pterygopalatine artery bifurcation via an external carotid artery stump. Reperfusion was performed by withdrawing the suture 60 min after the occlusion. All of the mice were killed at 3 d of reperfusion, except the chronic groups of IRF5 and IRF4 CKO mice that were examined 30 d after stroke. Sham-operated animals underwent the same surgical procedure, but the suture was not advanced into the internal carotid artery. The size of the MCAO-induced infarct was measured by triphenyltetrazolium chloride (TTC) or cresyl violet (CV) staining as described in refs. 44 and 45. Behavior deficits after stroke were evaluated by neurological deficit scores (10, 46), corner test (47, 48), hanging wire test (49), adhesive removal test (50, 51), Y-maze spontaneous alternation test (52, 53), and novel object recognition test (NORT) (54–56). Details of these behavior tests are contained in *SI Appendix*.

Flow Cytometry. Tissue processing for flow cytometry was performed as previously described (10, 57). Briefly, phosphate-buffered saline perfused mice brains were placed in complete Roswell Park Memorial Institute 1640 (Lonza) medium and mechanically and enzymatically digested in 150 μL collagenase/dispase (1 mg/mL) and 300 μL DNase (10 mg/mL; both Roche Diagnostics) for 45 min at 37 °C with mild agitation. Harvested cells were washed and blocked with mouse Fc Block (eBioscience) prior to staining with primary antibody-conjugated fluorophores (eBioscience): CD45-eF450, CD11b-AF488, Ly6C-APC-eF780, Ly6G-PE, MHCII-APC, and CD206-PE-cy5.5. For live/dead cell discrimination, a fixable viability dye, carboxylic acid succinimidyl ester (AF350, Invitrogen), was used. Data were acquired on a CytoFLEX (Beckman Coulter) and analyzed using FlowJo (Treestar). For intracellular cytokine staining, an ex vivo brefeldin A protocol was followed (10, 58), and an intracellular antibody mixture (0.25 μg for each antibody, 1:100 dilution) containing TNFα-PE-Cy7 (eBioscience) and IL-1β-PE (eBioscience), IL-10-APC, and IL-4-PerCP-Cy5.5 (BioLegend) was used for staining. In flow-sorted microglia, RT-PCR was performed by using the RNAqueous-Micro Total RNA Isolation Kit (Thermo Fisher Scientific). The primer sequences are as follows: Forward IRF4—5′-CAAAGCACAGAGTCACCTGG-3′; Reverse IRF4: 5′-CTGCCCTGTCAGAGTATTTC-3′; Forward IRF5—5′-CCTCAGCCGTACAAGATCTACGA-3′; Reverse IRF5—5′-GTAGC-ATTCTCTGGAGCTCTTCCT-3′; Forward—GAPDH: 5′-GTGTTCCTACCCCCAATGTGT-3′; Reverse GAPDH—5′ ATTGTCATACCAGGAAATGAGCTT-3′.

Lentivirus Administration In Vivo. Custom lentiviral vectors encoding IRF4 or IRF5 tagged with enhanced green fluorescent protein under the control of the CX3CR1 promoter specifically for microglia were bought from Genecopoei (Rockville, MD). The lenti-IRF5 or -IRF4 was injected into mice brains with a stereotaxic apparatus following previously established methods (59, 60). Briefly, a 4-point injection was carried out at the following coordinates: 0.5 mm anterior to the bregma, 2.0 or 3.0 mm lateral (right) to the sagittal suture, and 1.0 or 2.8 mm from the surface of the skull. A total of 1.0 μL of concentrated lentivirus (10^9 transducing units/mL) was injected into each site at a rate of 0.2 μL/min with a 30-gauge needle on a 10-μL Hamilton syringe (catalog #80010) for 5 min. After the lentivirus was injected, the needle remained in position for 5 min before it was withdrawn. This injection protocol causes minimal damage to the brain tissue according to our previous experience. Lenti-GFP served as the control. After 4 wk of lentivirus microinjection, mice were subjected to either sham or stroke surgery.

MultiPlex and Enzyme-Linked Immunosorbent Assay. Cytokine levels in plasma and the supernatant of cell cultures were measured by commercially available specific MultiPlex quantitative Bio-Plex Pro Mouse Cytokine 23-plex assay

according to the manufacturer's instruction (# M60009RDPD, Bio-Rad Laboratories, Hercules, CA) except for TNF-α and IL-4 that were measured by commercially available specific quantitative sandwich Enzyme-Linked Immunosorbent Assay (ELISA) kits (# 430904, 431104, BioLegend, San Diego).

Statistical Analysis. Data from individual experiments were presented as mean ± SD and assessed by Student's *t* test or 1-way ANOVA or 2-way ANOVA with Tukey post hoc test for multiple comparisons (GraphPad Prism Software, San Diego) except NDS, which was analyzed with the Mann–Whitney *U* test. Data from the corner test were analyzed by 2-way ANOVA, and significant differences between paired comparisons were confirmed with the Holm–Sidak test. Significance was set at $P < 0.05$.

Data Availability. All data discussed in the paper are available in the main text or *SI Appendix*.

ACKNOWLEDGMENTS. This work was supported by funding from NIH Grants R01 NS093042/NS108779 (to F.L.) and R37 NS096493 (to L.D.M.).

1. A. Rayasam *et al*., Immune responses in stroke: How the immune system contributes to damage and healing after stroke and how this knowledge could be translated to better cures? *Immunology* **154**, 363–376 (2018).
2. P. Devarajan, Z. Chen, Autoimmune effector memory T cells: The bad and the good. *Immunol. Res.* **57**, 12–22 (2013).
3. J. V. Faustino *et al*., Microglial cells contribute to endogenous brain defenses after acute neonatal focal stroke. *J. Neurosci.* **31**, 12992–13001 (2011).
4. M. Lalancette-Hébert, G. Gowing, A. Simard, Y. C. Weng, J. Kriz, Selective ablation of proliferating microglial cells exacerbates ischemic injury in the brain. *J. Neurosci.* **27**, 2596–2605 (2007).
5. X. Hu *et al*., Microglia/macrophage polarization dynamics reveal novel mechanism of injury expansion after focal cerebral ischemia. *Stroke* **43**, 3063–3070 (2012).
6. A. R. Patel, R. Ritzel, L. D. McCullough, F. Liu, Microglia and ischemic stroke: A double-edged sword. *Int. J. Physiol. Pathophysiol. Pharmacol.* **5**, 73–90 (2013).
7. G. Szalay *et al*., Microglia protect against brain injury and their selective elimination dysregulates neuronal network activity after stroke. *Nat. Commun.* **7**, 11499 (2016).
8. W. N. Jin *et al*., Depletion of microglia exacerbates postischemic inflammation and brain injury. *J. Cereb. Blood Flow Metab.* **37**, 2224–2236 (2017).
9. R. Günthner, H. J. Anders, Interferon-regulatory factors determine macrophage phenotype polarization. *Mediators Inflamm.* **2013**, 731023 (2013).
10. A. Al Mamun *et al*., Interferon regulatory factor 4/5 signaling impacts on microglial activation after ischemic stroke in mice. *Eur. J. Neurosci.* **47**, 140–149 (2018).
11. C. Cunha, C. Gomes, A. R. Vaz, D. Brites, Exploring new inflammatory biomarkers and pathways during LPS-induced M1 polarization. *Mediators Inflamm.* **2016**, 6986175 (2016).
12. T. Aratake *et al*., The inhibitory role of intracellular free zinc in the regulation of Arg-1 expression in interleukin-4-induced activation of M2 microglia. *Metallomics* **10**, 1501–1509 (2018).
13. J. E. Rehg, D. Bush, J. M. Ward, The utility of immunohistochemistry for the identification of hematopoietic and lymphoid cells in normal tissues and interpretation of proliferative and inflammatory lesions of mice and rats. *Toxicol. Pathol.* **40**, 345–374 (2012).
14. M. Cross, I. Mangelsdorf, A. Wedel, R. Renkawitz, Mouse lysozyme M gene: Isolation, characterization, and expression studies. *Proc. Natl. Acad. Sci. U.S.A.* **85**, 6232–6236 (1988).
15. H. J. Kim *et al*., Deficient autophagy in microglia impairs synaptic pruning and causes social behavioral defects. *Mol. Psychiatry* **22**, 1576–1584 (2017).
16. M. Pulido-Salgado *et al*., Myeloid C/EBPβ deficiency reshapes microglial gene expression and is protective in experimental autoimmune encephalomyelitis. *J. Neuroinflammation* **14**, 54 (2017).
17. X. Zhang *et al*., Macrophage/microglial Ezh2 facilitates autoimmune inflammation through inhibition of Socs3. *J. Exp. Med.* **215**, 1365–1382 (2018).
18. E. Butturini, D. Boriero, A. Carcereri de Prati, S. Mariotto, STAT1 drives M1 microglia activation and neuroinflammation under hypoxia. *Arch. Biochem. Biophys.* **669**, 22–30 (2019).
19. E. Bok *et al*., Modulation of M1/M2 polarization by capsaicin contributes to the survival of dopaminergic neurons in the lipopolysaccharide-lesioned substantia nigra in vivo. *Exp. Mol. Med.* **50**, 76 (2018).
20. C. Porro, A. Cianciulli, T. Trotta, D. D. Lofrumento, M. A. Panaro, Curcumin regulates anti-inflammatory responses by JAK/STAT/SOCS signaling pathway in BV-2 microglial cells. *Biology (Basel)* **8**, E51 (2019).
21. S. Monga, R. Nagler, R. Amara, A. Weizman, M. Gavish, Inhibitory effects of the two novel TSPO ligands 2-Cl-MGV-1 and MGV-1 on LPS-induced microglial activation. *Cells* **8**, E486 (2019).
22. A. Aguzzi, C. Zhu, Microglia in prion diseases. *J. Clin. Invest.* **127**, 3230–3239 (2017).
23. N. Rimmerman, N. Schottlender, R. Reshef, N. Dan-Goor, R. Yirmiya, The hippocampal transcriptomic signature of stress resilience in mice with microglial fractalkine receptor (CX3CR1) deficiency. *Brain Behav. Immun.* **61**, 184–196 (2017).
24. C. Bertot, L. Groc, E. Avignone, Role of CX3CR1 signaling on the maturation of GABAergic transmission and neuronal network activity in the neonate Hippocampus. *Neuroscience* **406**, 186–201 (2019).
25. S. Lively, L. C. Schlichter, Microglia responses to pro-inflammatory stimuli (LPS, IFNγ+TNFα) and reprogramming by resolving cytokines (IL-4, IL-10). *Front. Cell. Neurosci.* **12**, 215 (2018).
26. K. E. Hawkins *et al*., Targeting resolution of neuroinflammation after ischemic stroke with a lipoxin A_4 analog: Protective mechanisms and long-term effects on neurological recovery. *Brain Behav.* **7**, e00688 (2017).
27. X. Hu *et al*., Microglial and macrophage polarization: New prospects for brain repair. *Nat. Rev. Neurol.* **11**, 56–64 (2015).
28. R. A. Taylor, L. H. Sansing, Microglial responses after ischemic stroke and intracerebral hemorrhage. *Clin. Dev. Immunol.* **2013**, 746068 (2013).
29. K. Honda, T. Taniguchi, IRFs: Master regulators of signalling by Toll-like receptors and cytosolic pattern-recognition receptors. *Nat. Rev. Immunol.* **6**, 644–658 (2006).
30. A. Takaoka *et al*., Integral role of IRF-5 in the gene induction programme activated by Toll-like receptors. *Nature* **434**, 243–249 (2005).
31. D. T. Clarke, N. A. McMillan, Gene delivery: Cell-specific therapy on target. *Nat. Nanotechnol.* **9**, 568–569 (2014).
32. M. C. Milone, U. O'Doherty, Clinical use of lentiviral vectors. *Leukemia* **32**, 1529–1541 (2018).
33. R. A. Taylor *et al*., TGF-β1 modulates microglial phenotype and promotes recovery after intracerebral hemorrhage. *J. Clin. Invest.* **127**, 280–292 (2017).
34. A. N. vonderEmbse, Q. Hu, J. C. DeWitt, Dysfunctional microglia:neuron interactions with significant female bias in a developmental gene x environment rodent model of Alzheimer's disease. *Int. Immunopharmacol.* **71**, 241–250 (2019).
35. K. M. Gillen, M. Mubarak, T. D. Nguyen, D. Pitt, Significance and *in vivo* detection of iron-laden microglia in white matter multiple sclerosis lesions. *Front. Immunol.* **9**, 255 (2018).
36. R. Liu *et al*., BpV(pic) confers neuroprotection by inhibiting M1 microglial polarization and MCP-1 expression in rat traumatic brain injury. *Mol. Immunol.* **112**, 30–39 (2019).
37. J. Liu *et al*., Post-stroke treatment with argon attenuated brain injury, reduced brain inflammation and enhanced M2 microglia/macrophage polarization: A randomized controlled animal study. *Crit. Care* **23**, 198 (2019).
38. R. M. Ritzel *et al*., Aging alters the immunological response to ischemic stroke. *Acta Neuropathol.* **136**, 89–110 (2018).
39. T. Goldmann *et al*., A new type of microglia gene targeting shows TAK1 to be pivotal in CNS autoimmune inflammation. *Nat. Neurosci.* **16**, 1618–1626 (2013).
40. C. I. Tasca, T. Dal-Cim, H. Cimarosti, In vitro oxygen-glucose deprivation to study ischemic cell death. *Methods Mol. Biol.* **1254**, 197–210 (2015).
41. L. D. McCullough *et al*., Pharmacological inhibition of AMP-activated protein kinase provides neuroprotection in stroke. *J. Biol. Chem.* **280**, 20493–20502 (2005).
42. C. B. Moore, E. H. Guthrie, M. T. Huang, D. J. Taxman, Short hairpin RNA (shRNA): Design, delivery, and assessment of gene knockdown. *Methods Mol. Biol.* **629**, 141–158 (2010).
43. J. Wang *et al*., CXCR6 induces prostate cancer progression by the AKT/mammalian target of rapamycin signaling pathway. *Cancer Res.* **68**, 10367–10376 (2008).
44. F. Liu, D. P. Schafer, L. D. McCullough, TTC, fluoro-Jade B and NeuN staining confirm evolving phases of infarction induced by middle cerebral artery occlusion. *J. Neurosci. Methods* **179**, 1–8 (2009).
45. L. D. McCullough *et al*., Stroke sensitivity in the aged: Sex chromosome complement vs. gonadal hormones. *Aging (Albany N.Y.)* **8**, 1432–1441 (2016).
46. F. Liu, S. E. Benashski, Y. Xu, M. Siegel, L. D. McCullough, Effects of chronic and acute oestrogen replacement therapy in aged animals after experimental stroke. *J. Neuroendocrinol.* **24**, 319–330 (2012).
47. X. Li *et al*., Chronic behavioral testing after focal ischemia in the mouse: Functional recovery and the effects of gender. *Exp. Neurol.* **187**, 94–104 (2004).
48. B. Manwani *et al*., Functional recovery in aging mice after experimental stroke. *Brain Behav. Immun.* **25**, 1689–1700 (2011).
49. S. Ji *et al*., Acute neuroprotection by pioglitazone after mild brain ischemia without effect on long-term outcome. *Exp. Neurol.* **216**, 321–328 (2009).
50. T. Freret *et al*., Behavioral deficits after distal focal cerebral ischemia in mice: Usefulness of adhesive removal test. *Behav. Neurosci.* **123**, 224–230 (2009).
51. O. Mohamad *et al*., Vector-free and transgene-free human iPS cells differentiate into functional neurons and enhance functional recovery after ischemic stroke in mice. *PLoS One* **8**, e64160 (2013).
52. K. K. Hsiao *et al*., Age-related CNS disorder and early death in transgenic FVB/N mice overexpressing Alzheimer amyloid precursor proteins. *Neuron* **15**, 1203–1218 (1995).
53. A. K. Swonger, R. H. Rech, Serotonergic and cholinergic involvement in habituation of activity and spontaneous alternation of rats in a Y maze. *J. Comp. Physiol. Psychol.* **81**, 509–522 (1972).
54. D. A. Christakis, J. S. Ramirez, J. M. Ramirez, Overstimulation of newborn mice leads to behavioral differences and deficits in cognitive performance. *Sci. Rep.* **2**, 546 (2012).
55. I. Gallo *et al*., Formyl peptide receptor as a novel therapeutic target for anxiety-related disorders. *PLoS One* **9**, e114626 (2014).
56. G. Taglialatela, D. Hogan, W. R. Zhang, K. T. Dineley, Intermediate- and long-term recognition memory deficits in Tg2576 mice are reversed with acute calcineurin inhibition. *Behav. Brain Res.* **200**, 95–99 (2009).
57. A. Chauhan *et al*., Myeloid-specific TAK1 deletion results in reduced brain monocyte infiltration and improved outcomes after stroke. *J. Neuroinflammation* **15**, 148 (2018).
58. R. M. Ritzel *et al*., Multiparity improves outcomes after cerebral ischemia in female mice despite features of increased metabovascular risk. *Proc. Natl. Acad. Sci. U.S.A.* **114**, E5673–E5682 (2017).
59. L. Liu *et al*., Ras-related C3 botulinum toxin substrate 1 promotes axonal regeneration after stroke in mice. *Transl. Stroke Res.* **9**, 506–514 (2018).
60. H. Yuan *et al*., Nuclear translocation of histone deacetylase 4 induces neuronal death in stroke. *Neurobiol. Dis.* **91**, 182–193 (2016).